processes

MDPI

Article

Evaluation of the Thermal and Morphological Properties of γ-Irradiated Chitosan-Glycerol-Based Polymeric Films

Waheed A. Al-Masry [1,*], Sajjad Haider [1], Asif Mahmood [1], Mujeeb Khan [2], Syed Farooq Adil [2] and Mohammed Rafiq H. Siddiqui [2,*]

[1] Chemical Engineering Department, College of Engineering, King Saud University, P.O. Box 800, Riyadh 11421, Saudi Arabia; shaider@ksu.edu.sa (S.H.); ahayat@ksu.edu.sa (A.M.)
[2] Department of Chemistry, College of Science, King Saud University, P.O. Box 2455, Riyadh 11451, Saudi Arabia; kmujeeb@ksu.edu.sa (M.K.); sfadil@ksu.edu.sa (S.F.A.)
* Correspondence: walmasry@ksu.edu.sa (W.A.A.-M.); rafiqs@ksu.edu.sa (M.R.H.S.); Tel.: +966-11-467-0439 (M.R.H.S.)

Abstract: Industry-sponsored research has intensified to find suitable substitutes for synthetic polymers. For this purpose, biopolymers are promising materials that are extracted from renewable resources. However, there are areas of concern (biopolymers are mostly brittle in the dry state) that require further research before they are used in advanced applications. To overcome this, plasticizers are often added to biopolymers to enhance their physicochemical properties. In this study, chitosan (CH)-glycerol (GL)-based polymeric films were prepared by a simple drop-casting technique, and the influence of a plasticizer (GL) on the properties of chitosan films was analyzed. Additionally, the as-prepared samples were irradiated with γ-rays (^{60}Co γ rays with a dose of 10^2 kGy) to study the effect of γ-irradiation on the properties of polymeric composites. To achieve this, different samples were prepared by varying the amount of GL. FT-IR analysis revealed the interruption of hydrogen bonding in chitosan by the incorporation of GL. This led to the chain-spreading of CH, which ultimately increased the flexibility of the composite films (CH-GL). The DSC of the CH film showed two peaks: one endothermic peak below 100 °C (due to water vapor) and a second exothermic peak that appeared between 130 and 360 °C (degradation of the amino group). Plasticization of CH films with GL was confirmed by DSC, where the exothermic degradation was converted into an endothermic peak. Depending upon the amount of GL, γ-irradiation considerably affected the chemical structure of CH by breaking the carbohydrate and pyranose rings; this led to a decrease in the crystallinity of the composite films. The changes studied in the DSC and TGA analysis complemented each other. γ-irradiation also affected the morphology of the films, which changed from smooth and homogeneous to roasted structures, with random swelling on the surface of the films. This swelling reflected the degradation of the surfaces into thin layers. Considering the changes that occurred in the films post-γ-irradiation, it can be inferred that the irradiation dose of 10^2 kGy is sufficient to degrade as-prepared biopolymer composites.

Keywords: biopolymer; composite films; chitosan; plasticizer; glycerol; γ-irradiation

Citation: Al-Masry, W.A.; Haider, S.; Mahmood, A.; Khan, M.; Adil, S.F.; Siddiqui, M.R.H. Evaluation of the Thermal and Morphological Properties of γ-Irradiated Chitosan-Glycerol-Based Polymeric Films. *Processes* **2021**, *9*, 1783. https://doi.org/10.3390/pr9101783

Academic Editor: Katherine M. E. Stewart

Received: 25 August 2021
Accepted: 3 October 2021
Published: 7 October 2021

1. Introduction

Currently, global environmental issues with the growing use of non-biodegradable polymers in daily applications have led to an increased interest of researchers in finding sustainable alternatives from renewable sources [1,2]. In recent times, remarkable developments have occurred in the fabrication of films and coating materials, by employing polymers that are obtained from renewable, natural sources [3,4]. These polymers include cellulose, chitosan, alginate, and starch, which are beneficial in the packaging industry [5,6]. These materials act as a barrier to moisture, oil, vapor, etc., and are predicted to increase the shelf life of products when used as coating materials for protective packaging [7]. Among these polymers, chitosan has gained a prominent position due to its unique cationic nature

and easy processibility [8]. Chitosan is a natural, polycationic linear polysaccharide that is typically derived from abundantly available chitin through its partial deacetylation [9]. Chitin is a natural polymer obtained from the shells of crabs and shrimps, which are the major sources of waste in the seafood industry [10,11]. Chitosan is an abundant biopolymer, and after cellulose, is the second-most abundant natural polysaccharide. It is non-toxic, biodegradable, and biocompatible, and thus can be easily blended with other negatively charged synthetic or natural polymers, to obtain functional materials for various biological and biomedical applications [12,13].

Although chitosan is not soluble in an aqueous solution, its solubility can be significantly enhanced in acidic conditions [14]. The enhanced solubility of chitosan under acidic conditions is attributed to the formation of salt between the negative ions of acid and the protonated amino group of chitosan [15]. Due to its easy processibility, chitosan can be effectively used to make films, and therefore is considered a potential material for food packaging, especially edible films and coatings [16,17]. Usually, chitosan-based biofilms are transparent and non-porous; however, the wide-scale application of these films is often limited due to their brittle nature, and hence, they cannot be used in targeted packaging applications [18]. To overcome this issue, plasticizers are used to alter the polymer chain interactions, which are mainly responsible for the brittleness of these films [19,20].

To date, many natural plasticizers have been reported to enhance the plasticity of biopolymers, including sorbitol, glycerol, polyethylene glycol (PEG), etc. [21]. These materials can potentially enhance the flexibility and processibility of biopolymers by reducing the second-order transition temperature, specifically, the glass transition temperature (Tg) [22]. Usually, plasticizers have low molecular weights (between 300 and 600 kDa) and are high-boiling liquids, consisting of linear or cyclic carbon chains, which intercalate the polymer matrix and reduce secondary forces among them [23,24]. Thereby, these molecules alter the three-dimensional structure of polymer matrices, which reduces the energy requirement for molecular motion and the formation of hydrogen bonding between the chains [25]. Consequently, the amount of free volume available in the polymer matrix increases significantly, which enhances molecular mobility in the sample [26,27]. Among various plasticizers, glycerol (GL) is considered a good plasticizer for use in biopolymer-based films, which is known to enhance the barrier and mechanical properties of biodegradable polymer films [28–30].

The properties of polymeric materials, including biodegradable polymer-based composite films, can be customized by several techniques, including variation of the composite ratio, doping, ion beam-related methods, etc., to obtain desirable functional properties for certain applications [31,32]. Among these methods, customization by ion beam and radiation treatment are techniques that have the potential to effectively calibrate the physicochemical, surface, and structural properties of polymeric materials [33,34]. Particularly, these materials are very sensitive to gamma radiation, which has been exploited for the modification, degradation, and sterilization of polymeric materials [35]. Upon irradiation with gamma rays, polymers demonstrate various effects, such as crosslinking or reticulation, degradation or scission of polymeric chains, depending on the structure of the polymer, irradiation dose, additive concentration, and irradiation conditions (atmosphere and temperature) [36]. So far, few studies have reported the effects of gamma irradiation on the properties of chitosan-based polymeric films. The synthesis of chitosan oligomers via irradiation, both in solid and solution state [37], evaluation of the effect on the molecular weight and physical properties of chitosan films by irradiation with ^{60}Co gamma rays were previously reported [38]. Similarly, the effect of irradiation with ^{60}Co (10, 25, 50, and 100 kGy) on the mechanical properties of films obtained from irradiated chitosan derived from prawns was also reported [39].

To the best of our knowledge, no study on the effect of gamma irradiation and the concentration of glycerol plasticizer on the physicochemical properties of chitosan-glycerol composite films has been reported. Therefore, considering the potential of biodegradable polymers in various fields, pre-and post-irradiation analysis of changes that occur in

biopolymer films is highly desirable. This investigation aimed to demonstrate the effect of gamma irradiation and the amount of plasticizer on the structure, and biodegradation of the chitosan-glycerol blend.

2. Materials and Methods

2.1. Materials

Medium molecular weight (190–130 k Da) chitosan powder $(C_8H_{13}NO_5)n$ (CH), acetic acid ($(C_2H_4O_2)$ AcOH), and glycerol (GL) as a plasticizer were purchased from Sigma-Aldrich (Missouri, USA). All chemicals were of analytical grade and were used without further purification. Distilled water was used for the preparation of solutions.

2.2. Preparation of the Film

Chitosan solutions at 2 wt % concentration were prepared by dissolving a calculated amount of chitosan (Table 1) in 2 wt % ACOH using a magnetic stirrer (model Cerastir 30539) at 45 °C for 2 h. After complete dissolution, solutions were filtered through a mesh with 0.063 mm pore size to obtain a homogeneous solution and remove any undissolved particles. The homogeneous solution of CH was placed on the stirrer and a calculated amount of GL was added dropwise to the solution using a micropipette. The solution was further stirred for 3 h at room temperature. Finally, the composite solution was cast in Petri dishes. The casted solution was left to dry at room temperature. After drying, the films were peeled and stored for characterization (Figure 1).

Table 1. Composition of CH and GL composite films.

Sample Code	Chitosan (g)	Glycerol (g)	Ratio	Film Removed from Petri Dish
CH	2	0	100/0	Yes
CH-GL-1	1.8	0.2	90/10	Yes
CH-GL-2	1.6	0.4	80/20	Yes
CH-GL-3	1.2	0.6	60/40	Yes
CH-GL4	1	1	50/50	No

Figure 1. Digital images of the solution casting of the (**A**) chitosan (CH) and CH-GL films, (**B**) dried stored films, and (**C**) illustrating the flexibility of CH-GL film.

2.3. Characterization

2.3.1. Morphology

The surface morphologies of the CH and CH-GL films were investigated under high vacuum through SEM (VEGA TESCAN, Libušina, Czech Republic). The samples were fixed on the holder with double-sided sticking tape and were coated with platinum in a platinum-sputtering machine to increase their electrical conductivities and create contrast between the sample and background. Finally, micrographs of the films were taken at constant magnifications.

2.3.2. FT-IR Study

The FT-IR spectra of CH and CH-GL films were obtained using an FT-IR spectrometer (Bruker Vertex 70, Billerica, MA, USA). The samples were analyzed in film form

by separately placing them into the FT-IR machine. The spectra were acquired in the 400–4000 cm^{-1} range.

2.3.3. XRD Study

The amorphous and crystalline behavior of the CH and CH-GL films was determined by an X-ray diffractometer (Bruker AXS D8 Advance XRD, Billerica, MA, USA). The XRD data were obtained at 40 kV and 30 mA using Cu Kα radiation (1.540 Å). We studied 2θ° in the range of 20° to 80°.

2.3.4. DSC Study

The miscibility and crystallinity of CH and CH-GL were studied by a differential scanning calorimeter ((DSC) Q20, TA Instruments, New Castle, DE, USA). The samples were placed in the heating compartment and heated at 5 °C/min from 25 to 350 °C in an air environment, and the thermogram was recorded.

2.3.5. TGA

The thermal behavior of the CH and CH-GL films was studied using TGA (Q50, TA Instruments, New Castle, DE, USA). The samples were placed in the platinum plate, weighed, and heated at 10 °C/min in the temperature range (Tr) of 25 to 600 °C under a N_2 environment, and the degradation pattern of the films was recorded.

2.3.6. Radiation Study

For irradiation of the films, polymeric samples were encapsulated under a vacuum in glass vials and were successively exposed to increasing doses of radiation at a constant intensity using C-60 γ-ray cell 220 (Nordion International Inc., Ottawa, ON, Canada) at a dose rate of 10^4 Gyh^{-1}. In this study, the samples were irradiated at a dose of 10^2 kGy at ambient temperature (~20 °C). Irradiations were performed at the Research Centre Lab, Department of Chemistry, King Saud University, Riyadh, KSA.

3. Results and Discussion

3.1. FT-IR Studies

The influence of GL on the CH films was analyzed using FT-IR. Figure 2 shows the spectra of pristine CH and the post-irradiated CH films. The spectrum of chitosan exhibited all of the characteristic bands reported in the literature. The bands at 2910 and 2867 cm^{-1} are assigned to the asymmetric vibrations of CH_2 in the carbohydrate ring. The band in the range of 1330 to 1420 cm^{-1} is the characteristic band of the C–N stretching of amide, vibrations of CH_2 in the carbohydrate ring, and O-H bending. The band at 896 cm^{-1} is assigned to the C–O–C of the glycosidic linkage [40]. The medium primary N-H bending band is observed in the range of 1580 to 1550 cm^{-1}. After irradiation, the FT-IR spectrum of the CH film (blue line, Figure 2) was similar to the spectrum of a non-irradiated sample, with some minor changes; the band in the range of 1330 to 1420 cm^{-1}, belonging to in-plane bending of –OH and CH_2 in the carbohydrate ring, was missing in the irradiated sample, possibly due to disruption in the polymer network. Pristine GL had a wide range of bands between 600 and 3000 cm^{-1}, which are mostly attributed to the stretching of O–H bonds, with either inter- or intramolecular hydrogen bonds. These bands could also be formed by water molecules, whose angular deformation was seen at 1651 cm^{-1} [41]. The FT-IR spectra of different samples of CH-GL before and after irradiation were also measured, which were prepared by varying the amount of GL, as shown in Table 1 and Figure 3. As evident from the spectra of CH-GL, after mixing CH and GL, the IR bands in CH-GL did not change considerably compared to the IR bands of pristine CH; however, the band intensity at 1330 to 1420 cm^{-1}, assigned to the in-plane bending of –OH and CH_2 in the carbohydrate ring, was slightly influenced by the addition of GL. This indicates that the addition of GL into CH interrupted hydrogen bonding, thereby spreading the chains and increasing the flexibility of the composite films (CH-GL). Notably, γ-irradiation

had a considerable effect on the structural properties of the composite films, which varied according to film composition. For example, in CH-GL films, the band around 1420 cm^{-1}, attributed to the in-plane bending of –OH and CH_2 in the carbohydrate ring, disappeared in the irradiated samples. Similarly, the intensity of the band at 896 cm^{-1}, attributed to the glycosidic linkage C–O–C of the carbohydrate ring units, decreased significantly. As shown in Figure 3, a similar effect was also observed in all CH-GL samples (CH-GL-1, CH-GL-2, CH-GL-3, and CH-GL-4). It is noteworthy that at a lower concentration of GL (CH-GL-1), not only did the band at 1330 to 1420 cm^{-1} disappear, but the intensity of the 896 cm^{-1} band also decreased. In the sample containing a high amount of GL (CH-GL-3), only the intensities of these two bands decreased. From these results, it can be concluded that irradiation affected/degraded the chemical structure (Scheme 1) of the CH and CH-GL samples by breaking the carbohydrate and pyranose rings.

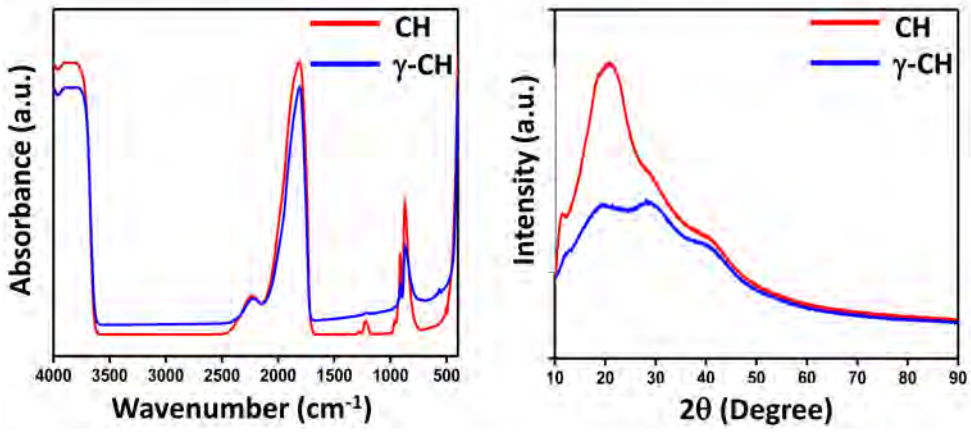

Figure 2. FT-IR spectra and XRD spectra of chitosan and γ-irradiated chitosan.

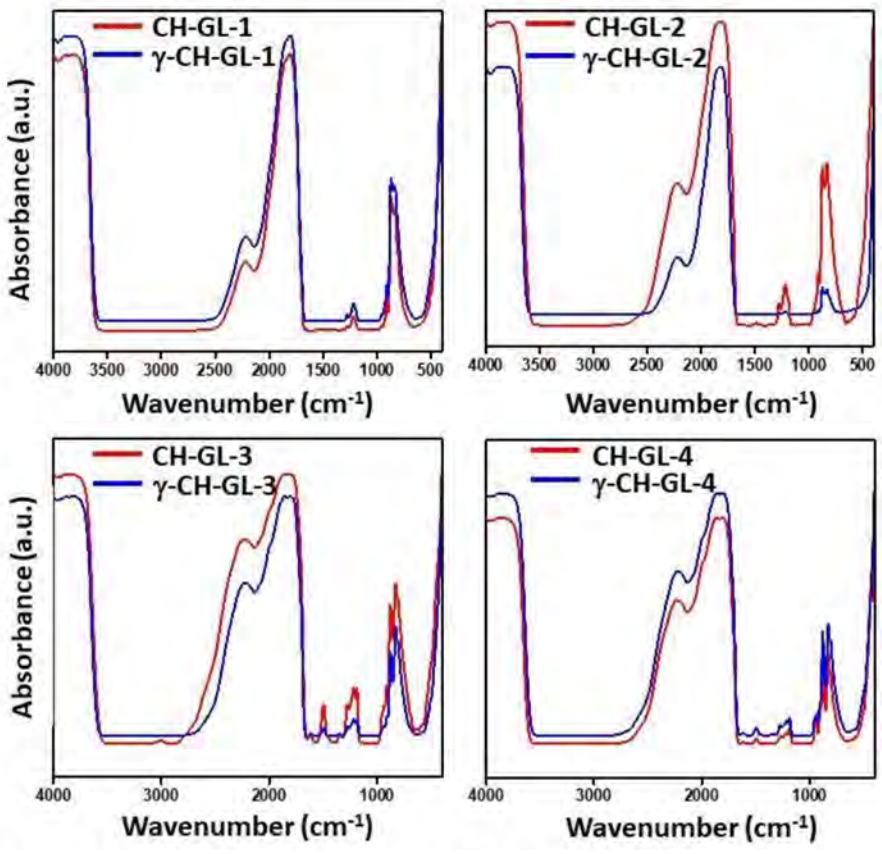

Figure 3. FT-IR spectra of the chitosan-gly film before and after γ-irradiation.

Scheme 1. Proposed degradation pathway of plasticized chitosan after irradiation.

3.2. XRD Study

Figure 4 illustrates the XRD patterns of pre-and post-irradiated CH-GL samples. The characteristic XRD patterns of pristine CH (cf. Figure 4) showed broad diffraction bands at a 2θ of 20° due to its amorphous characteristics. The characteristics of crystalline bands in WAXD patterns, reported in the literature, showed comparable crystallinity for the two types (alpha chitosan and gamma chitosan), with a consistent peak in XRD at 20° [42]. The XRD patterns of plasticized CH-GL films also illustrated similar bands in the same region (2θ = 20°), as shown in Figure 4.

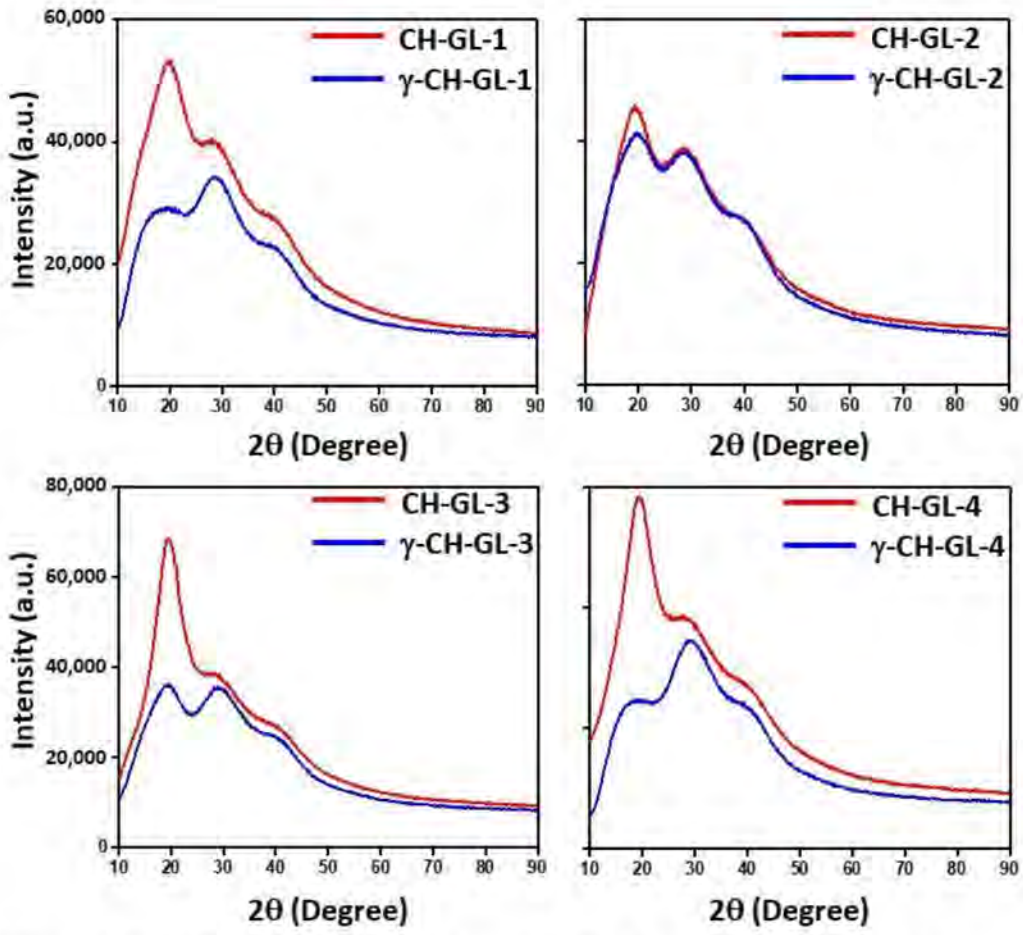

Figure 4. XRD diffraction spectra of the chitosan-gly films before and after γ-irradiation.

However, the intensity of this band varied by the change in the amount of GL in the composite films. These changes in the diffraction band intensities showed that the addition of plasticizer (GL) interrupted the inter-and intra-hydrogen bonding, which led to the unpacking of the molecular chains. This opening of the chain packing resulted in a further decrease in the crystallinity of the samples. In addition to plasticizers, irradiation had a significant effect on the XRD patterns of the samples; the single broad diffraction band of CH separated into two bands (20° and 30°) in the CH-GL composite films. In addition, the intensity of the band at 20° decreased, and its peak became broader. The broad, low-intensity band at 30° is assigned to GL. These changes in the diffraction peaks revealed that though glycerol showed some effect on the crystallinity of CH, the major effect, however, was achieved by irradiation. Contrarily, upon calculating the degree of crystallinity (DC) by deconvoluting the XRD spectra of the samples and the area of the amorphous and crystalline bands by the following formula, opposite results were obtained [43,44].

$$D_c = \frac{A_C}{A_T}\ A_C\ = \text{Sum of area of crystalline peaks};\ A_T\ = \text{Sum of area of all peaks (amorphous and crystalline peaks)} \quad (1)$$

Calculations revealed that the crystallinity of the composite varied with the addition of plasticizer, and upon irradiation, the crystallinity increased (which is opposite to the results obtained from other characterizations including SEM and FTIR), and this increase in crystallinity ratio was the maximum for the CH film, i.e., CH (Figure 5). Furthermore, as the ratio of plasticizer increased from 10 to 20 i.e., CH-GL-1 and CH-GL-2, the crystallinity decreased from 21% to 14%, respectively, and upon irradiation, the crystallinity of the same was found to be 53% and 17%, respectively. However, upon further increase in plasticizer in the film to 40–50, i.e., CH-GL-3 and CH-GL-4, the crystallinity increased from 28% to 33%, respectively, and upon irradiation, the crystallinity increased to 49% and 61%, respectively.

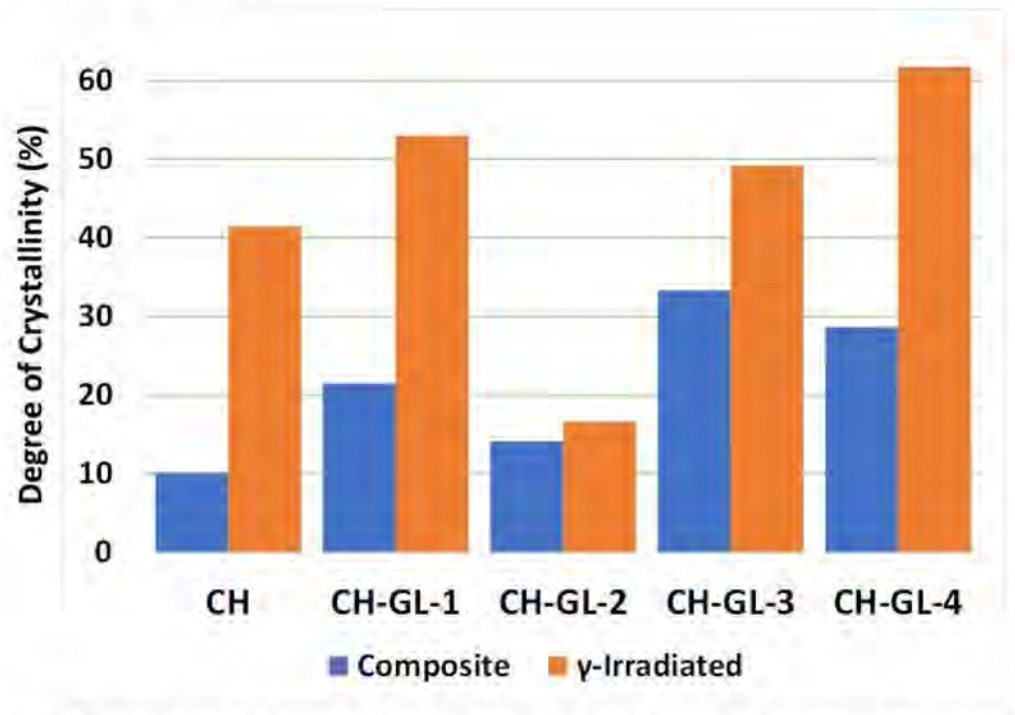

Figure 5. Illustration of changes in the crystallinity of the chitosan film before and after γ-irradiation.

Crystallinity measurements from XRD deconvolution are a popular approach; however, it has been found that the crystallinity index varies significantly depending on the choice of the measurement method. Furthermore, it was reported that the simplest and most widely used method, which involves the measurement of just two peaks in the X-

ray diffractogram (as performed in this study), sometimes produces significantly higher crystallinity values than other methods [45]. Therefore, in this study, the increased crystallinity of the samples after irradiation could be due to an error in the calculation of the crystallinity index from the XRD deconvolution method, as the results obtained from other techniques, including FT-IR, SEM, and DSC, indicate degradation of the samples after treatment with gamma rays. Irradiation affected the hydrogen bonds within the structure of the CH-GL network, leading to lower crystallinity [46]. Furthermore, the FT-IR spectra showed damage to the chemical structure, which could be another factor in lowering the crystallinity of the CH.

3.3. Morphology

The surface morphologies of CH and CH-GL films were determined using SEM. The micrographs are shown in Figure 6. SEM micrographs of pristine CH (cf. Figure 6) and all samples of the CH-GL films (cf. Figure 7) revealed the presence of smooth and homogeneous surface morphologies, indicating the miscibilities of CH and GL.

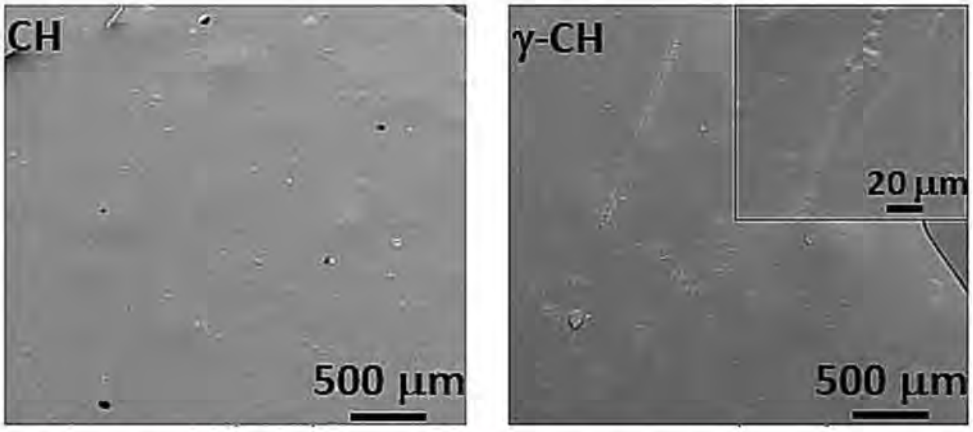

Figure 6. SEM images of the chitosan film before and after γ-irradiation.

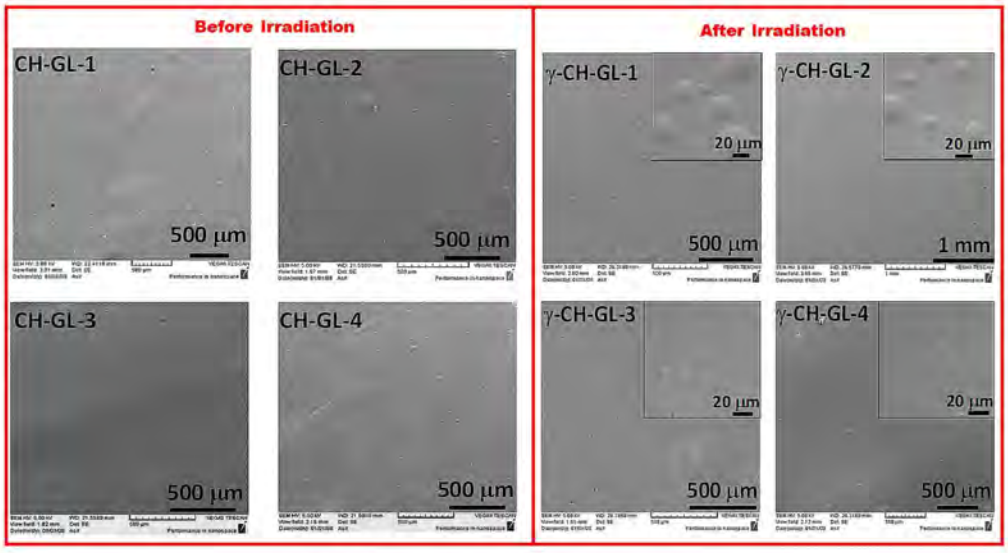

Figure 7. SEM micrographs of the chitosan-gly films before and after irradiation.

There was neither aggregation of any particulate matter, pores (the black spots in some micrographs were due to some dust on the films), nor phase separation (the materials were not segregated from each other). The absence of phase separation in the SEM micrographs is clear evidence that both CH and GL mixed at the micro-level. These results are in

agreement with those reported in the literature [47]. As mentioned in the Introduction section, GL penetrated the CH chains and interrupted hydrogen bonds (both inter-and intramolecular), spreading the chains to make the polymer more flexible and plastic, with a continuous phase (no phase separation). The continuous phase was also confirmed by the appearance of the signal Tg (Table 2) in the DSC results for all samples.

Table 2. Tg, melting point, degradation, and crystallization of the composite samples before and after irradiation.

	Sample Name	Tg (°C)	Mt/dt (°C)	Enthalpy (J/G)	Crystallinity (%)
Before irradiation	**CH**	**188.55**	**269.26**	**−63.60**	**NA**
	CH-GL-1	**177.31**	**265.90**	**−6.598**	**NA**
	CH-GL-2	**173.46**	**269.70**	**−29.34**	**NA**
	CH-GL-3	**141.70**	**246.64**	**93.23**	**32.15**
	CH-GL-4	**133.10**	**247.55**	**96.28**	**33.20**
After γ-irradiation	**γ-CH**	**145.68**	**261.38**	**−74.52**	**NA**
	γ-CH-GL1	**141.81**	**267.38**	**−87.90**	**NA**
	γ-CH-GL-2	**139.31**	**267.96**	**−91.01**	**NA**
	γ-CH-GL-3	**134.40**	**244.93**	**87.58**	**30.20**
	γ-CH-GL-4	**179.30**	**249.44**	**84.67**	**29.19**

Radiation treatments demonstrated a concentration (GL)-dependent effect on the surface morphologies of CH-GL films. For example, the smooth surfaces of CH and CH-GL-3 converted into rough surfaces following irradiation. Similarly, the surfaces of CH-GL-1, CG-GL-2, and CH-GL-4 showed roasted structures, where swelling of the surface was observed. This swelling shows the breaking of the surfaces into thin layers, as shown in Figure 7 [48,49].

3.4. Thermal Properties

The DSC and TGA thermograms of non-irradiated and irradiated pristine CH and its blends with GL are shown in Figures 8a–d and 9, respectively. The DSC of CH and its blends' films showed an interesting thermal phenomenon. Figure 8a,c is broken down into three parts to aid in the interpretation and understanding of this phenomenon. The first phase contained peaks at temperatures that are lower than 100 °C. The second phase displayed endo-peaks for the blends (B3P and B4P), while the third phase displayed degradation of CH and its blends B1P and B12P. The evaporation of water is related to the peak in the first phase that appeared below 100 °C. Peaks in the third phase are attributed to a thermal event due to amine unit degradation in CH, with an exothermic peak [50]. As stated, an unusual and interesting thermal event was noticed when the GL percentage of the mixture was increased: the degradation peak transformed into the melting peak. This change in degradation peak to melting peak with increasing GL percentage can be attributed to the rearrangement of CH chains in the presence of GL, which may have resulted in some crystallinity. This assumption was verified after the determination of the percent crystallinity. The percent crystallinity increased as the GL percentage in the blend increased. The glass transition temperature (Tg) of CH and its mixtures is shown in Figure 8c. Figure 8 and Table 2 show that as the GL percentage in the blend increased, Tg and melting temperature (mt) dropped. This is evidence of the plasticization effect. The irradiated CH and its blends (Figure 8c,d) also showed the same three phases in the DSC thermogram and the plasticization effect. It should be noted, however, that Tg was substantially lowered in irradiated blends compared to non-irradiated blends. These findings imply that the bonding between polymer chains was altered not only by GL, but also by radiation exposure. TGA also followed the same pattern. The degradation of the films began above 130 °C and reached its maximum at ~360 °C; in this temperature range, a large part of the composite film had degraded. No major shift was observed in the TGA thermogram. Both DSC and TGA analyses were in agreement (cf. Figure 9).

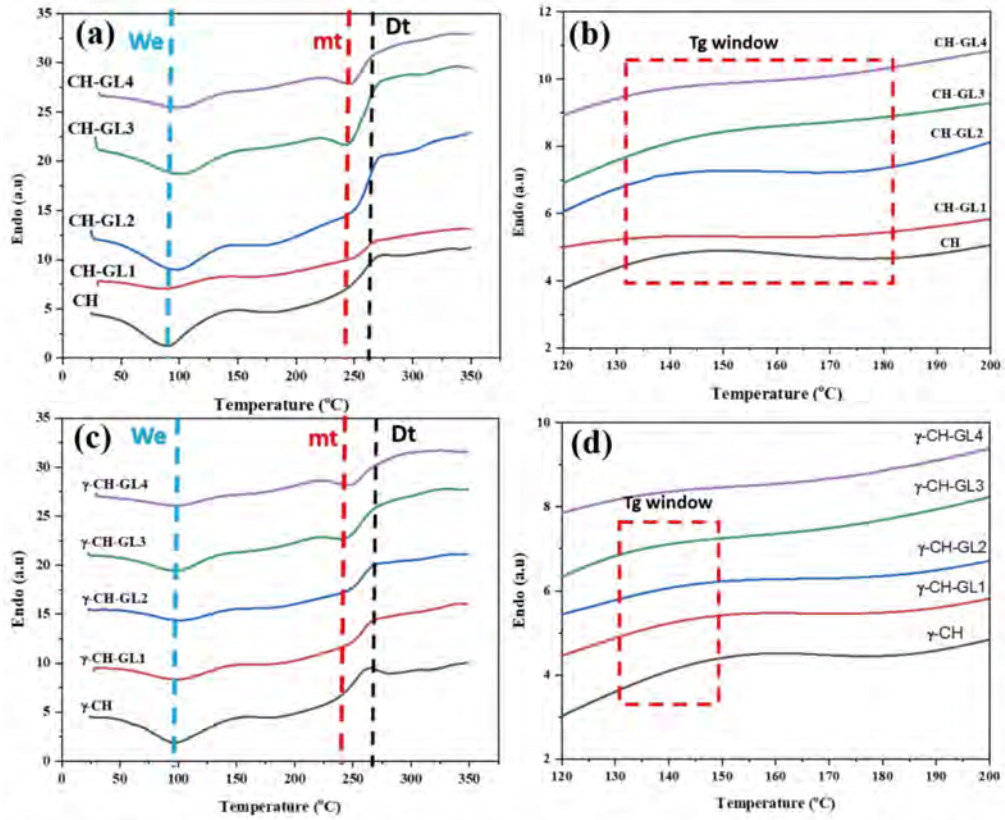

Figure 8. DSC thermogram of the CH and its blend with GL, (**a**,**b**) nonirradiated and (**c**,**d**). Note: "We" indicates water evaporation, mt is melting temperature, and dt is degradation temperature.

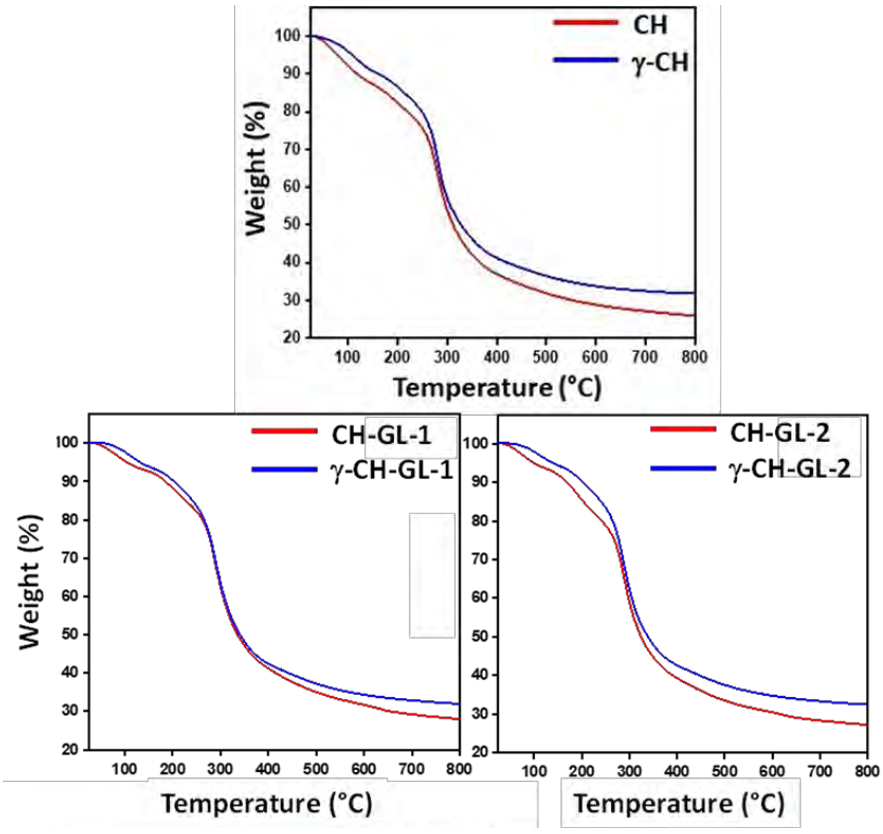

Figure 9. *Cont*.

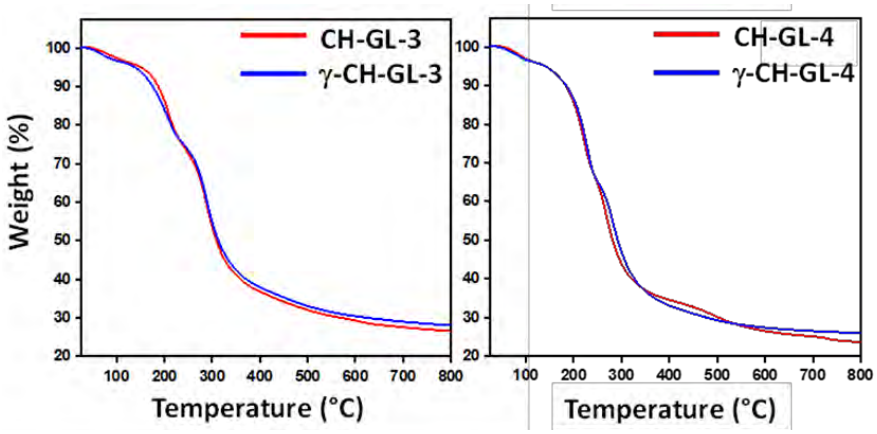

Figure 9. TGA thermogram of the CH-GL films before and after γ-irradiation.

4. Conclusions

Herein, we successfully demonstrated the preparation of plasticizer-incorporated CH-GL composite films to enhance the flexibility of the biopolymer and studied the γ-irradiation effect on the properties of these films. Plasticizer (GL) was found to have a positive effect on the structure of CH films. The addition of GL interrupted inter-and intra-hydrogen bonding, which led to the unpacking and rearrangement of the molecular chains that resulted in the conversion of exothermal degradation into endothermal melting. Furthermore, the films became flexible and showed a continuous phase (no phase separation was confirmed by the single Tg in the DSC results). Irradiation affected the chemical structure of the samples, which resulted in decreased crystallinity. Irradiation also affected film morphology, which changed to roasted, where swelling of the surface was observed. This swelling indicated the breaking of the surfaces into thin layers. The degradation of the films started above 150 °C and reached its maximum at 360 °C. The changes studied in the DSC and TGA complemented each other. Therefore, the incorporation of plasticizer enhanced the flexibility of the as-prepared films, whereas γ-irradiation facilitated the degradation of composite films.

Author Contributions: W.A.A.-M. and M.R.H.S. designed the project; S.H., A.M., M.K. and S.F.A. helped to write the manuscript; S.H. and A.M. performed the experimental section and some part of characterization; M.K. and S.F.A. performed some part of characterization; W.A.A.-M. and M.R.H.S. provided scientific guidance for the successful completion of the project and helped to draft the manuscript. All authors have read and agreed to the published version of the manuscript.

Funding: The authors extend their appreciation to the Deputyship for Research & Innovation, Ministry of Education in Saudi Arabia for funding this research work through the project number DRI-KSU-637.

Institutional Review Board Statement: Not applicable.

Informed Consent Statement: Not applicable.

Data Availability Statement: Data are contained within the article.

Acknowledgments: The authors extend their appreciation to the Deputyship for Research & Innovation, Ministry of Education in Saudi Arabia for funding this research work through the project number DRI-KSU-637.

Conflicts of Interest: The authors declare no conflict of interest.

References

1. Zhu, Y.; Romain, C.; Williams, C.K. Sustainable polymers from renewable resources. *Nature* **2016**, *540*, 354–362. [CrossRef]
2. Agarwal, S. Biodegradable Polymers: Present Opportunities and Challenges in Providing a Microplastic-Free Environment. *Macromol. Chem. Phys.* **2020**, *221*, 2000017. [CrossRef]

3. Bulatović, V.O.; Mandić, V.; Grgić, D.K.; Ivančić, A. Biodegradable polymer blends based on thermoplastic starch. *J. Polym. Environ.* **2021**, *29*, 492–508. [CrossRef]
4. Mellinas, C.; Ramos, M.; Jiménez, A.; Garrigós, M.C. Recent trends in the use of pectin from agro-waste residues as a natural-based biopolymer for food packaging applications. *Materials* **2020**, *13*, 673. [CrossRef] [PubMed]
5. Kraśniewska, K.; Galus, S.; Gniewosz, M. Biopolymers-based materials containing silver nanoparticles as active packaging for food applications—A review. *Int. J. Mol. Sci.* **2020**, *21*, 698. [CrossRef]
6. Mangaraj, S.; Yadav, A.; Bal, L.M.; Dash, S.; Mahanti, N.K. Application of biodegradable polymers in food packaging industry: A comprehensive review. *J. Packag. Technol. Res.* **2019**, *3*, 77–96. [CrossRef]
7. Negm, N.A.; Hefni, H.H.; Abd-Elaal, A.A.; Badr, E.A.; Abou Kana, M.T. Advancement on modification of chitosan biopolymer and its potential applications. *Int. J. Biol. Macromol.* **2020**, *152*, 681–702. [CrossRef]
8. Sahariah, P.; Masson, M. Antimicrobial chitosan and chitosan derivatives: A review of the structure–activity relationship. *Biomacromolecules* **2017**, *18*, 3846–3868. [CrossRef]
9. Muxika, A.; Etxabide, A.; Uranga, J.; Guerrero, P.; De La Caba, K. Chitosan as a bioactive polymer: Processing, properties and applications. *Int. J. Biol. Macromol.* **2017**, *105*, 1358–1368. [CrossRef]
10. El Knidri, H.; Belaabed, R.; Addaou, A.; Laajeb, A.; Lahsini, A. Extraction, chemical modification and characterization of chitin and chitosan. *Int. J. Biol. Macromol.* **2018**, *120*, 1181–1189. [CrossRef]
11. Zhao, D.; Yu, S.; Sun, B.; Gao, S.; Guo, S.; Zhao, K. Biomedical applications of chitosan and its derivative nanoparticles. *Polymers* **2018**, *10*, 462. [CrossRef]
12. Kravanja, G.; Primožič, M.; Knez, Ž.; Leitgeb, M. Chitosan-based (Nano) materials for novel biomedical applications. *Molecules* **2019**, *24*, 1960. [CrossRef] [PubMed]
13. Rui, L.; Xie, M.; Hu, B.; Zhou, L.; Saeeduddin, M.; Zeng, X. Enhanced solubility and antioxidant activity of chlorogenic acid-chitosan conjugates due to the conjugation of chitosan with chlorogenic acid. *Carbohydr. Polym.* **2017**, *170*, 206–216. [CrossRef] [PubMed]
14. Qin, Y.; Li, P.; Guo, Z. Cationic chitosan derivatives as potential antifungals: A review of structural optimization and applications. *Carbohydr. Polym.* **2020**, *236*, 116002. [CrossRef]
15. Cazón, P.; Vázquez, M. Applications of chitosan as food packaging materials. In *Sustainable Agriculture Reviews 36*; Springer: Berlin/Heidelberg, Germany, 2019; pp. 81–123.
16. Kumar, S.; Mukherjee, A.; Dutta, J. Chitosan based nanocomposite films and coatings: Emerging antimicrobial food packaging alternatives. *Trends Food Sci. Technol.* **2020**, *97*, 196–209. [CrossRef]
17. Hänninen, A.; Sarlin, E.; Lyyra, I.; Salpavaara, T.; Kellomäki, M.; Tuukkanen, S. Nanocellulose and chitosan based films as low cost, green piezoelectric materials. *Carbohydr. Polym.* **2018**, *202*, 418–424. [CrossRef]
18. Chen, M.; Runge, T.; Wang, L.; Li, R.; Feng, J.; Shu, X.-L.; Shi, Q.-S. Hydrogen bonding impact on chitosan plasticization. *Carbohydr. Polym.* **2018**, *200*, 115–121. [CrossRef]
19. Sacco, P.; Cok, M.; Asaro, F.; Paoletti, S.; Donati, I. The role played by the molecular weight and acetylation degree in modulating the stiffness and elasticity of chitosan gels. *Carbohydr. Polym.* **2018**, *196*, 405–413. [CrossRef]
20. Toxqui-Terán, A.; Leyva-Porras, C.; Ruíz-Cabrera, M.Á.; Cruz-Alcantar, P.; Saavedra-Leos, M.Z. Thermal study of polyols for the technological application as plasticizers in food industry. *Polymers* **2018**, *10*, 467. [CrossRef]
21. Ibrahim, M.; Sapuan, S.; Zainudin, E.; Zuhri, M. Physical, thermal, morphological, and tensile properties of cornstarch-based films as affected by different plasticizers. *Int. J. Food Prop.* **2019**, *22*, 925–941. [CrossRef]
22. El Miri, N.; Aziz, F.; Aboulkas, A.; El Bouchti, M.; Ben Youcef, H.; El Achaby, M. Effect of plasticizers on physicochemical properties of cellulose nanocrystals filled alginate bionanocomposite films. *Adv. Polym. Technol.* **2018**, *37*, 3171–3185. [CrossRef]
23. O'zeren, H.s.D.; Guivier, M.; Olsson, R.T.; Nilsson, F.; Hedenqvist, M.S. Ranking Plasticizers for Polymers with Atomistic Simulations: PVT, Mechanical Properties, and the Role of Hydrogen Bonding in Thermoplastic Starch. *ACS Appl. Polym. Mater.* **2020**, *2*, 2016–2026. [CrossRef]
24. Aliotta, L.; Vannozzi, A.; Panariello, L.; Gigante, V.; Coltelli, M.-B.; Lazzeri, A. Sustainable micro and nano additives for controlling the migration of a biobased plasticizer from PLA-based flexible films. *Polymers* **2020**, *12*, 1366. [CrossRef] [PubMed]
25. Chen, J.; Li, K.; Wang, Y.; Huang, J.; Nie, X.; Jiang, J. Synthesis and properties of a novel environmental epoxidized glycidyl ester of ricinoleic acetic ester plasticizer for poly (vinyl chloride). *Polymers* **2017**, *9*, 640. [CrossRef]
26. Rodríguez-Núñez, J.R.; Madera-Santana, T.J.; Sánchez-Machado, D.I.; López-Cervantes, J.; Valdez, H.S. Chitosan/hydrophilic plasticizer-based films: Preparation, physicochemical and antimicrobial properties. *J. Polym. Environ.* **2014**, *22*, 41–51. [CrossRef]
27. Zanjanijam, A.R.; Hakim, S.; Azizi, H. Migration of the plasticizer in the compatibilized PP/PVB blends: Characterization and thermodynamic calculations. *Polym. Bull.* **2018**, *75*, 4671–4689. [CrossRef]
28. Lavorgna, M.; Piscitelli, F.; Mangiacapra, P.; Buonocore, G.G. Study of the combined effect of both clay and glycerol plasticizer on the properties of chitosan films. *Carbohydr. Polym.* **2010**, *82*, 291–298. [CrossRef]
29. Ferreira, F.; Dufresne, A.; Pinheiro, I.; Souza, D.; Gouveia, R.; Mei, L.; Lona, L. How do cellulose nanocrystals affect the overall properties of biodegradable polymer nanocomposites: A comprehensive review. *Eur. Polym. J.* **2018**, *108*, 274–285. [CrossRef]
30. Escárcega-Galaz, A.A.; Sánchez-Machado, D.I.; López-Cervantes, J.; Sanches-Silva, A.; Madera-Santana, T.J.; Paseiro-Losada, P. Mechanical, structural and physical aspects of chitosan-based films as antimicrobial dressings. *Int. J. Biol. Macromol.* **2018**, *116*, 472–481. [CrossRef]

31. Kobielarz, M.; Gazińska, M.; Tomanik, M.; Stępak, B.; Szustakiewicz, K.; Filipiak, J.; Antończak, A.; Pezowicz, C. Physicochemical and mechanical properties of CO2 laser-modified biodegradable polymers for medical applications. *Polym. Degrad. Stab.* **2019**, *165*, 182–195. [CrossRef]
32. Terakawa, M. Femtosecond laser processing of biodegradable polymers. *Appl. Sci.* **2018**, *8*, 1123. [CrossRef]
33. Shibata, A.; Yada, S.; Terakawa, M. Biodegradability of poly (lactic-co-glycolic acid) after femtosecond laser irradiation. *Sci. Rep.* **2016**, *6*, 27884. [CrossRef]
34. Patel, G.B.; Singh, N.; Singh, F. Modification of chitosan-based biodegradable polymer by irradiation with MeV ions for electrolyte applications. *Mater. Sci. Eng. B* **2017**, *225*, 150–159. [CrossRef]
35. Sabaghi, M.; Maghsoudlou, Y.; Kashiri, M.; Shakeri, A. Evaluation of release mechanism of catechin from chitosan-polyvinyl alcohol film by exposure to gamma irradiation. *Carbohydr. Polym.* **2020**, *230*, 115589. [CrossRef] [PubMed]
36. Kodal, M.; Wis, A.A.; Ozkoc, G. The mechanical, thermal and morphological properties of γ-irradiated PLA/TAIC and PLA/OvPOSS. *Radiat. Phys. Chem.* **2018**, *153*, 214–225. [CrossRef]
37. Hai, L.; Diep, T.B.; Nagasawa, N.; Yoshii, F.; Kume, T. Radiation depolymerization of chitosan to prepare oligomers. *Nucl. Instrum. Methods Phys. Res. Sect. B Beam Interact. Mater. At.* **2003**, *208*, 466–470. [CrossRef]
38. García, M.A.; Pérez, L.; de la Paz, N.; González, J.; Rapado, M.; Casariego, A. Effect of molecular weight reduction by gamma irradiation on chitosan film properties. *Mater. Sci. Eng. C* **2015**, *55*, 174–180. [CrossRef] [PubMed]
39. Zainol, I.; Akil, H.M.; Mastor, A. Effect of γ-irradiation on the physical and mechanical properties of chitosan powder. *Mater. Sci. Eng. C* **2009**, *29*, 292–297. [CrossRef]
40. Zhuang, J.; Li, M.; Pu, Y.; Ragauskas, A.J.; Yoo, C.G. Observation of potential contaminants in processed biomass using fourier transform infrared spectroscopy. *Appl. Sci.* **2020**, *10*, 4345. [CrossRef]
41. Guimarães, J.L.; Trindade Cursino, A.C.; Ketzer Saul, C.; Sierrakowski, M.R.; Ramos, L.P.; Satyanarayana, K.G. Evaluation of castor oil cake starch and recovered glycerol and development of "Green" composites based on those with plant fibers. *Materials* **2016**, *9*, 76. [CrossRef] [PubMed]
42. Ogawa, K.; Hirano, S.; Miyanishi, T.; Yui, T.; Watanabe, T. A new polymorph of chitosan. *Macromolecules* **1984**, *17*, 973–975. [CrossRef]
43. Arafat, A.; Samad, S.A.; Masum, S.M.; Moniruzzaman, M. Preparation and characterization of chitosan from shrimp shell waste. *Int. J. Sci. Eng. Res.* **2015**, *6*, 538–541.
44. Ioelovich, M. Crystallinity and hydrophility of chitin and chitosan. *J. Chem.* **2014**, *3*, 7–14.
45. Park, S.; Baker, J.O.; Himmel, M.E.; Parilla, P.A.; Johnson, D.K. Cellulose crystallinity index: Measurement techniques and their impact on interpreting cellulase performance. *Biotechnol. Biofuels* **2010**, *3*, 1–10. [CrossRef]
46. Hao, G.; Hu, Y.; Shi, L.; Chen, J.; Cui, A.; Weng, W.; Osako, K. Physicochemical characteristics of chitosan from swimming crab (Portunus trituberculatus) shells prepared by subcritical water pretreatment. *Sci. Rep.* **2021**, *11*, 1646. [CrossRef]
47. Kumar, R.; Mishra, I.; Kumar, G. Synthesis and Evaluation of Mechanical Property of Chitosan/PVP Blend through Nanoindentation-A Nanoscale Study. *J. Polym. Environ.* **2021**, *29*, 3770–3778. [CrossRef]
48. Ziani, K.; Oses, J.; Coma, V.; Maté, J.I. Effect of the presence of glycerol and Tween 20 on the chemical and physical properties of films based on chitosan with different degree of deacetylation. *LWT-Food Sci. Technol.* **2008**, *41*, 2159–2165. [CrossRef]
49. Rivero, S.; García, M.; Pinotti, A. Composite and bi-layer films based on gelatin and chitosan. *J. Food Eng.* **2009**, *90*, 531–539. [CrossRef]
50. Ferrero, F.; Periolatto, M. Antimicrobial finish of textiles by chitosan UV-curing. *J. Nanosci. Nanotechnol.* **2012**, *12*, 4803–4810. [CrossRef]